LINC01272 Activates Epithelial-Mesenchymal Transition Through miR-153-5p in Crohn's Disease

Lin Fang
the affiliated hospital of nanjing medical university
Mengcheng Hu
the affiliated hospital of nanjing medical university
Fei Xia
The affiliated hospital of nanjing medical university
wenxia Bai (baiwenxia0213@126.com)
the affiliated hospital of nanjing medical university https://orcid.org/0000-0003-3870-2078

Research Article

Keywords: Crohn's disease, LINC01272, miR-153-5p, EMT

Posted Date: August 24th, 2021

DOI: https://doi.org/10.21203/rs.3.rs-746920/v1

Abstract

Background: Long non-coding RNAs (lncRNAs) have different functions in different diseases. There is seldom research on the functions of lncRNAs in Crohn's disease (CD). By RNA-seq technology, we identify a lncRNA associated with Crohn's disease. However, the mechanism of lncRNA regulation remains unknown. This study aimed to determine the association of LINC01272 with epithelial cell-mesenchymal transition and the underlined mechanism in CD.

Methods: RNA is detected by qRT-PCR. Interaction of protein and RNA was determined by RNA binding protein immunoprecipitation. Luciferase reporter assays were used to detect the targeted miRNA of LINC01272. Tissue fibrosis was observed by Masson and HE staining. The protein expression is determined by western blot and immunofluorescence.

Results: LINC01272 was highly expressed in patients with CD. Knockdown of LINC01272 inhibited TGF-β1-induced epithelial-mesenchymal transition (EMT). Additionally, LINC01272 regulated TGF-β1 induced EMT by miR-153-5p axis and knockdown of LINC01272 inhibited EMT in the CD mice *in vivo*.

Conclusion: LINC01272 activated epithelial-mesenchymal transition through miR-153-5p in CD.

Introduction

CD is an unexplained intestinal inflammatory disease that occurs in any part of the gastrointestinal tract, but it usually occurs in the terminal ileum and right colon[1–5]. Both CD and chronic nonspecific ulcerative colitis are collectively referred to as inflammatory bowel disease (IBD). The clinical manifestations of this disease are abdominal pain, diarrhea, intestinal obstruction, and extraintestinal manifestations such as fever and nutritional disorders[6,7]. The course of the disease is often protracted, recurrent, and it is not easy to cure. The common nosogenesis of CD includes genetic mutations, environmental factors, and personal immunity[8–10]. Under pathogenic conditions, intestinal mucosal cells undergo an EMT, and epithelial cells lose their polarity and intercellular adhesion[11,12]. Myofibroblasts with strong movement and migration ability also secrete large amounts of extracellular matrix (such as collagen-I, III). EMT has a dual effect on the formation of tissue fibrosis: (1) EMT increases the number of mesenchymal cells and matrix production; (2) EMT causes the loss of epithelial cells and increases tissue damage[13,14]. During this process, the expression of epithelial cell markers such as E-cadherin were decreased, and the expression of mesenchymal cell markers such as smooth muscle agonist protein (α-SMA), N-cadherin (N cadherin), and fibronectin increase[15–18].

Non-coding RNA (ncRNA) is currently one of the most popular research objects in the field of biomedicine[19,20]. Transcripts with a length of fewer than 200 nucleotides are called short non-coding RNAs, such as micro RNAs (miRNAs), RNAs (PIWI-interacting RNAs, piRNAs), and small interfering RNAs (Small Interfering RNAs, siRNAs)[21,22]. Another type of RNA that plays the role of miRNA sponge is called long non-coding RNAs (lncRNAs). LncRNA generally refers to the RNA with a greater than 200 nucleotides

in length and rarely participates in protein coding [23]. As competitive endogenous RNAs (ceRNAs), LncRNAs are able to be combined with miRNA and inhibit miRNA's effect on target genes and it locates in the nucleus or cytoplasm[24]. Its expression is tissue-specific and spatio-temporal specific. LINC01272, as a novel marker, has not been found in many studies.

In our finding, the purpose was to probe the functions of LINC01272 on CD and its potential mechanism. we found that LINC01272 activated EMT by regulating miR-153-5p expression in CD. Our study will provide an experimental basis for CD treatment and offer therapeutic targets against CD.

Methods

Clinical samples

Samples were taken from CD patients with colonic and ileal inflammatory lesions. Normal tissue was taken from healthy subjects undergoing colonoscopy. All samples were obtained from the affiliated Jiangning Hospital with Nanjing Medical University between October 2019 and October 2020. All participants had signed informed consent forms. Our experiments were approved by the ethic community of the affiliated Jiangning Hospital with Nanjing medical university. The clinical characteristics of CD and control patients are presented in **Table 1**.

Cell culture and transfection

IEC-6 cells (ATCC, Manassas, VA) were cultured with DMEM containing contained with 10% fetal bovine serum (FBS) at 5% CO_2, 37 °C. The shRNAs for LINC01272 as well as its corresponding scrambled siRNAs (sh-NC) were purchased by Hanbio (Shanghai, China). The miRNA oligonucleotides including miR-153-5p mimic, miR-153-5p inhibitor, NC mimic and NC inhibitor were obtained from RiboBio (Guangzhou, China). Transient transfection was performed by using Lipofectamine 3000 (Invitrogen, Carlsbad, CA, USA) according to the manufacturer's protocol. Cells were harvested 48-h post transfection for further experiment.

Establishment of CD mouse models

We used 2,4,6-trinitrobenzenesulfonic acid (TNBS) to construct the CD mouse model following the previous study [25]. Thirty female BALB/C mice were randomly divided into the control group (n=10), TNBS group (n = 10), and TNBS + sh-LINC01272 group (n = 10). The control group was fed a conventional diet, and the latter two groups were used TNBS (3.75 mg) to establish the CD model. Mice were shaved before the experiment and coated with TNBS 3.75 mg (dissolved in 48% ethanol). After fasting for 24-h, mice were narcotized using pentobarbital sodium on the 7th, 14th and 21st day after the coated TNBS, respectively. The trocar was inserted into the colon with a 20G trocar in the prone position, the top of which was about 4cm away from the anus. An ethanol solution of 100 μl TNBS was relaxedly injected into lumen immediately by a 1 ml syringe fixed with a trocar. In the third group, mice were injected intraperitoneally with 500μL sh-LINC01272. The blank control and the model group were treated with

same amount of saline. After the first treatment, the disease activity index (DAI) scores were recorded according to the previous report [26].

qRT-PCR analysis

Using Trizol to isolate RNA from cells or tissues. After the RNA was completely dissolved, the 5×PrimeScript® RT Master Mix kit was used for reverse transcription (10 μL). qRT-PCR was carried out by SYBR Premix Ex Taq TM (Takara, Otsu, Japan) on StepOnePlus™ Real-Time PCR System (Thermo Fisher Scientific). Here are the conditions of PCR reaction: Maintaining 94°C for 5 min, followed by 40 cycles at 94°C for 30 s, 55°C for 30 s, and 72°C for 60 s. The primers for qRT-PCR were shown in **Table 2**.

Western blot

Bicinchoninic Acid (BCA) kit (Wuhan Bost Biotechnology Company, Hubei, China) was used to extract the total proteins required for the experiment and detect its concentration. Then add 30 mg/well of loading buffer to the extracted proteins and boil it in a 95℃-water bath for 5 min After that, it was first separated by 10% polyacrylamide gel electrophoresis (Wuhan Bode Biotechnology, Hubei, China), and transferred to PVDF transmembrane (Millipore). Finally, the transferred transmembrane was placed in skim milk for 1 h. These bands were incubated with primary antibodies (1:1000, Abcam, MA, USA) at 4℃ overnight. Subsequently, these bands were treated with indicated secondary antibodies for 1-2 h. The dual-color infrared fluorescence scanning imaging system (Odyssey, Licor, NE, USA) was used to capture images, and then Image J 1.52v imaging analysis software (NIH, Bethesda, MD, USA) was used for analysis.

Immunofluorescence

IEC-6 cells were cultured in immunofluorescence-specific plates. Cells were washed using PBS and fixed in 4% paraformaldehyde for 20 min. Then cells were blocked with 0.1% BSA for 30 min at 23℃. Next, cells were followed by incubating with primary rabbit anti-collagen I (1:100 dilution) or rabbit anti-collagen III antibodies (1:100) overnight at 4°C. Alexa 555 secondary antibodies (Molecular Probes, Thermo Fisher Scientific, USA) and DAPI were used to incubate the cells. The cells were observed under a fluorescence microscope (Keyence, Ōsaka, Japan).

RNA Binding Protein Immunoprecipitation

The RIP experiment was carried out with the Magna RIP kit (Magna, ON, CAN). Briefly, the lysed cells were treated with the RIP buffer solution, and the magnetic beads were labeled using anti-Ago2 or IgG. The abundance of LINC01272 and miR-153-5p was verified by qRT-PCR.

Luciferase reporter assays

The promotor region of LINC01272 was cloned by PCR and inserted into the pGL3-LINC01272-WT and MUT plasmids through enzyme digestion to construct renilla luciferase vector. For the promotor region of LINC01272, the forward primer was “CGACUGACGCCG”, the reverse primer was “UCGACAUCGA”. The miR-

153-5p plasmids were co-transfected with pGL3-LINC01272 WT-renilla luciferase vector or pGL3-LINC01272 MUT-renilla luciferase vector into IEC-6 cells by Lipofectamine 2000 (Invitrogen). After the transfection plasmid was added to cells by the Lipofectamine 3000 (Invitrogen) for 48 h, the renilla luciferase in cell lysate was assessed by the dual-luciferase reporter assay system (BEST, Nanjing, China).

Masson staining

The tissue sections were stained with Masson's reagent according to the following procedures: (i) fixed in Bouin's or Zenker's liquor overnight, (ii) washed in running water until the yellow color fades and rinsed in distilled water for twice, (iii) stained with hematoxylin for 5 min, (iv) placed in 0.5% hydrochloric acid in 70% alcohol for 5 s, (v) washed for 30 s in running tap water and rinsed in distilled water for twice, (vi) stained with acid ponceau for 5-10 min and rinsed in distilled water for three times. Finally, cells were observed under a microscope.

HE staining

Briefly, the samples were dewaxed and hydrated with gradient alcohol, the sections were incubated in hematoxylin solution for 15 min followed washed with PBS. Secondly, the slices were counterstained with 0.5% eosin solution for 5 min, dehydrated with gradient alcohol, cleared, and sealed. Finally, photos were observed with light microscope (Keyence, Ōsaka, Japan).

Subcellular fraction

Cells were obtained in PBS and resuspended in ice 500 μL CLB buffer for 10 min. Homogenization was implemented by applying 15 strokes using a 1 ml needle on ice. Thereafter, 50 μl of 2.5M sucrose was added to restore isotonic conditions. The first round of centrifugation was implemented at 6300g for 5 min in a tabletop centrifuge at 4°C. The pellet washed with TSE buffer at 4000g for 6 min in a tabletop centrifuge at 4°C until the supernatant was clear. The resulting supernatant discarded and the pellets were nucleus. The resulting supernatant from the first round of differential centrifugation was sedimented for 150 min at 14000 rpm in a tabletop centrifuge. The resulting pellets were membranes and the supernatant was cytoplasm.

Wound-healing assay

All instruments are sterilized on the clean bench. Use a marker pen to draw a horizontal line 0.5~1cm from the back of the 6-well plate. At least 5 lines pass through each well. Add about 5*10^5 cells to the plate. The next day, use the tip of the pipette to make the scratch on the horizontal line. The tip of the pipette should be vertical and not inclined. Washing 3 times, serum-free medium was added into 6-well plate, and we put the plate into an incubator. Taking pictures at 0, 6, 12, and 24 h.

Transwell assay

The transwell membrane was covered with invasion matrigel. Briefly, the cells were plated on upper chambers with a serum-free medium at a density of 5 × 104 cells/well, while the bottom chamber was filled with medium with 10% FBS. After incubation for 24 h, the invaded cells were fixed with ice-cold methanol followed by staining with crystal violet (0.1%). Finally, the cells observed under a microscope (Olympus, Tokyo, Japan).

Bioinformatic prediction of lncRNA-miRNA interaction

The bioinformatics prediction was performed through the website: http://starbase.sysu.edu.cn/mirLncRNA.php.

Statistical analysis

All the results were presented as means ± SD. The significance between two groups was assessed by Unpaired Student's *t*-test or paired *t*-test, and multiple groups was evaluated by one-way ANOVA with Bonferroni post-hoc tests. $P < 0.05$ was considered significant.

Results

LINC01272 is highly expressed in CD.

A total of 60 samples were enrolled in this study, while 30 were diagnosed as CD patients, and the others constituted the control group. We collected 2ml peripheral blood of the patients and detected the LINC01272 expression. The results showed that in patients with CD, the expression of LINC01272 was dramatically higher than that of control group (Fig. 1A). Moreover, there was a positive correlation between the levels of LINC 01272 in tissue and plasma samples (Fig. 1B).

Knockdown of LINC01272 inhibits TGF-β1-stimulated EMT in IEC-6 cells.

Based on the high expression of LINC01272 in CD patients, we speculated that LINC01272 was involved in the development of non-specific intestinal inflammation. First, TGF-β1 was used to establish inflammatory cell model, found that TGF-β1 significantly promoted the expression of LINC01272 (Fig. 2A). Besides, sh-LINC01272 and its corresponding control were used to transfect IEC-6 cells. The transfection efficiency was shown in Fig. 2B, results revealed that the expression of LINC01272 was decreased in the sh-LINC01272 group. Next, we investigated the effect of LINC01272 on EMT, the main feature of CD progression, in TGF-β1 treated IEC-6 cells. The mRNA expression of E-cadherin and CK was decreased after TGF-β1 incubation in IEC-6, while knockdown of LINC01272 reversed the effect of TGF-β1 (Fig. 2C). In addition. TGF-β1 tremendously enhanced the levels of collagen I, collagen II, α-SMA and N-cadherin, which could be arrested by knockdown of LINC01272 (Fig. 2C). And the levels of protein detected by western blot and immunofluorescence presented the same trend as the expression of mRNA (Fig. 2D-E). Moreover, the result of wound-healing and transwell showed that TGF-β1 promoted the migrated ability and invasive ability, whereas which could be prevented by sh-LINC01272 (Fig. 2F-G). All these results demonstrated that LINC01272 silencing suppressed TGF-β1-induced EMT in IEC-6 cells.

MiR-153-5p targets 3' UTR of LINC01272.

After subcellular fraction, LINC01272 detected by qPCR was found mainly in the cytoplasm (Fig. 3A). Through bioinformatics software prediction, we found that miR-153-5p had pairing region targets 3'UTR of LINC01272 (Fig. 3B). Then, miR-153-5p mimic were used to treat cells, and qRT-PCR assay showed an increase of miR-153-5p in miR-153-5p mimic group (Fig. 3C). Luciferase reporter assays showed that the relative luciferase activity was high after pGL3-LINC01272 MUT-renilla luciferase vector and miR-153-5p mimic co-transfection compared to pGL3- LINC01272 WT-renilla luciferase vector and miR-153-5p mimic co-transfection, while no significant difference was observed when we replaced the miR-153-5p mimic with NC mimic (Fig. 3D). RIP assay showed that the relative enrichment of LINC01272 and miR-153-5p bound with Ago2 were high compared with IgG (Fig. 3E). Besides, the relative expression of miR-153-5p in the blood of CD patients and the IEC-6 cells after TGF-β1 treatment is lower than the control group (Fig. 3F-G). And knockdown of LINC01272 enhanced miR-153-5p expression (Fig. 3H). Pearson's correlation analysis showed that the expression of miR-153-5p was negatively correlated with that of LINC01272 (Fig. 3I).

LINC01272 regulates TGF-β1 induced EMT by miR-153-5p axis.

To figure out whether EMT regulated by LINC01272 was related to miR-153-5p, sh-LINC01272, and miR-153-5p inhibitor were used to transfect the TGF-β1-treated IEC-6 cells. As illustrated by the results of qPCR, inhibition of miR-153-5p obstructed the positive effect of sh-LINC01272 on the expression of E-cadherin and CK in TGF-β1-treated IEC-6 cells (Fig. 4A). Meanwhile, knockdown of miR-153-5p reversed a decrease of collagen I, collagen II, α-SMA and N-cadherin expression caused by sh- LINC01272 in TGF-β1-treated IEC-6 cells (Fig. 4A). In addition, the expression of protein detected by western blot presented the same trend as the expression of mRNA (Fig. 4B). Immunofluorescence assay revealed that the low expression of collagen I and collagen II caused by sh-LINC01272 was reversed by miR-153-5p inhibitor in TGF-β1-treated IEC-6 cells (Fig. 4C). The result of wound-healing and transwell showed that sh-LINC01272 inhibited the migrated ability and invasive ability of TGF-β1-treated IEC-6 cells, while inhibition of miR-153-5p could rescue the negative influence of sh-LINC01272 (Fig. 4D-E).

Knockdown of LINC01272 inhibits EMT in the CD mice in vivo.

We constructed a mouse model by using TNBS and evaluated the DAI score to research the relationship between LINC01272 and EMT *in vivo*. As showed in Fig. 5A, the DAI score of the TNBS + sh-LINC01272 group dropped over time since the 3rd week, while no downward trend in other groups. Histologically, HE staining showed that the colonic mucosa of the normal control group was intact, and the intestinal glands composed of a single layer of columnar epithelium, lamina propria, and mucosal muscular layer were clearly arranged. In the TNBS group, crypts were destroyed, goblet cells decreased, and epithelial cells were broken. Erosion, ulcer, and inflammatory cell infiltration at various levels of colon tissue mainly located in the mucosa and submucosa, and most infiltration cells were lymphocytes and monocytes, that is, the histological changes of chronic colitis. Damaged colon tissue could also be observed in the TNBS + sh-LINC01272 group, but the area and scope and the degree of inflammatory cell infiltration are lighter

than those in the TNBS group (Fig. 5B). In addition, Masson staining shows that in the TNBS group, a large amount of blue-stained collagen could be detected in the submucosa and serosal area, and there is occasionally fibrous separation. The colon tissue of mice in the TNBS + sh-LINC01272 group also showed a certain amount of scattered collagen fibers deposited in the above area. While the fibers were less than those of the TNBS group. The normal control group did not show the above performance (Fig. 5B). At the protein and mRNA levels, TNBS inhibited E-cadherin and CK expression, promoted collagen I, collagen II, α-SMA and N-cadherin expression, while sh-LINC01272 partly reversed the effects of TNBS (Fig. 5C-5E).

Discussion

Epithelial cell-mesenchymal transition (EMT) intends the biological process of epithelial cells transforming into cells with a mesenchymal phenotype through a specific process [27]. It plays an important role in embryonic development, chronic inflammation, tissue remodeling, cancer metastasis and various fibrotic diseases[28]. Through EMT, epithelial cells lose cell polarity and their connection with the basement membrane but acquire mesenchymal phenotypes such as high migration or invasion, anti-apoptosis, and the ability to degrade extracellular matrix. According to biological characteristics and biological markers, EMT is divided into 3 subtypes currently. Type 1 is related to embryo and organ formation. Type 2 is related to wound healing, tissue regeneration and organ fibrosis. Type 3 is related to tumor progression and metastasis[29]. Many clinical studies have determined that many different organ epithelial cells are transformed into myofibroblasts and fibroblast phenotypes through EMT leading to tissue fibrosis, such as renal tubules, lens epithelial cells, alveolar epithelial cells, and peritoneal mesothelial cells[30–32].

Inflammatory bowel diseases include CD and ulcerative colitis. One of its main complications is intestinal stricture caused by fibrosis of the intestinal wall. Intestinal wall fibrosis is due to excessive deposition of extracellular matrix during chronic inflammation and repair of intestinal damage. CD is more likely to produce fibrosis than ulcerative colitis[33]. CD is a chronic non-specific intestinal disease whose etiology and pathogenesis are unknown so far. In CD patients, the migration potential of myofibroblasts decreases. Epithelial cell migration, which could be induced by several growth factors, is another sign of intestinal mucosal repair[34]. If fibroblasts cannot cover the damaged tissue, epithelial cells will migrate here. After stimulating effects such as injury, inflammation, and hypoxia, inflammatory and fibrogenic mediators could be activated, which could induce the EMT procedure. In our study, TGF-β1 was used to induce EMT. After the treatment of TGF-β1, the ability to produce large amounts of collagen and fibronectin is obtained and the migration and penetration capabilities of cells are also changed.

LncRNAs played critical roles in biological processes, such as proliferation, metabolism, differentiation, and apoptosis, whereas altered expression levels contributed to the occurrence of diseases[35]. It is previously reported that LINC01272 accelerates the gastric cancer cells migration by EMT[36,37]. Similarly, we found that the levels of LINC01272 was elevation in CD patients. Furthermore, downregulation of

LINC01272 suppressed the epithelial cells migration and invasion. The variation of specific markers showed that LINC01272 induced EMT procedure. Therefore, LINC01272 was a potential determinant to prevent the endothelial. The crosstalk between lncRNAs and miRNAs is common in various diseases[38,39]. MiR-153-5p plays a critical role in LINC01272 regulation on EMT. These data enriched our knowledge of the functionality of miR-153-5p. However, EMT was caused by TGF-β1 *in vitro* or TNBS *in vivo* in this study, we should make a further investigation to figure out whether the effect of LINC01272 was applicable to EMT caused by other factors like genomic variants.

In conclusion, LINC01272 was upregulated, while miRNA-153-5p was downregulated in patients with CD. Our study found that LINC01272 activated EMT through miR-153-5p. This finding contributed to the current understanding of the role of LINC01272 in inflammatory bowel disease and provided a new therapeutic target.

Declarations

Acknowledgements

Ethics approval and consent to participate

This research was approved by the ethic community of the affiliated Jiangning Hospital with Nanjing medical university.

Consent for publication

Approved by all authors.

Availability of data and materials

N/A

Competing interests

The authors declare no conflicts of interests.

Authors' contributions

Wenxia Bai conceived the idea and led the manuscript writing. Lin Fang, Mengcheng Hu and Fei Xia all contributed equally to the work.

Funding

Supprotted by Medical Scientific Research Project of Jiangsu Commission of Health（project number： H2018081）and Science and Technology Development Project of Jiangning District（project number： 2018Ca07）

References

1. Torres, J., Mehandru, S., Colombel, J. F. & Peyrin-Biroulet, L. Crohn's disease. *Lancet* **389**, 1741-1755, doi:10.1016/S0140-6736(16)31711-1 (2017).
2. Ballester Ferre, M. P., Bosca-Watts, M. M. & Minguez Perez, M. Crohn's disease. *Med Clin (Barc)* **151**, 26-33, doi:10.1016/j.medcli.2017.10.036 (2018).
3. Harb, W. J. Crohn's Disease of the Colon, Rectum, and Anus. *Surg Clin North Am* **95**, 1195-1210, vi, doi:10.1016/j.suc.2015.07.005 (2015).
4. Chan, W. P. W., Mourad, F. & Leong, R. W. Crohn's disease associated strictures. *J Gastroenterol Hepatol* **33**, 998-1008, doi:10.1111/jgh.14119 (2018).
5. Li, J. *et al.* Pathogenesis of fibrostenosing Crohn's disease. *Transl Res* **209**, 39-54, doi:10.1016/j.trsl.2019.03.005 (2019).
6. Veauthier, B. & Hornecker, J. R. Crohn's Disease: Diagnosis and Management. *Am Fam Physician* **98**, 661-669 (2018).
7. Schneider, S. L., Foster, K., Patel, D. & Shwayder, T. Cutaneous manifestations of metastatic Crohn's disease. *Pediatr Dermatol* **35**, 566-574, doi:10.1111/pde.13565 (2018).
8. Chen, Y., Wang, Y. & Shen, J. Role of environmental factors in the pathogenesis of Crohn's disease: a critical review. *Int J Colorectal Dis* **34**, 2023-2034, doi:10.1007/s00384-019-03441-9 (2019).
9. Huang, R. T. *et al.* TBX20 loss-of-function mutation responsible for familial tetralogy of Fallot or sporadic persistent truncus arteriosus. *Int J Med Sci* **14**, 323-332, doi:10.7150/ijms.17834 (2017).
10. Li, N. & Shi, R. H. Updated review on immune factors in pathogenesis of Crohn's disease. *World J Gastroenterol* **24**, 15-22, doi:10.3748/wjg.v24.i1.15 (2018).
11. Lovisa, S., Genovese, G. & Danese, S. Role of Epithelial-to-Mesenchymal Transition in Inflammatory Bowel Disease. *J Crohns Colitis* **13**, 659-668, doi:10.1093/ecco-jcc/jjy201 (2019).
12. Bataille, F. *et al.* Evidence for a role of epithelial mesenchymal transition during pathogenesis of fistulae in Crohn's disease. *Inflamm Bowel Dis* **14**, 1514-1527, doi:10.1002/ibd.20590 (2008).
13. Kim, K. K. *et al.* Alveolar epithelial cell mesenchymal transition develops in vivo during pulmonary fibrosis and is regulated by the extracellular matrix. *Proc Natl Acad Sci U S A* **103**, 13180-13185, doi:10.1073/pnas.0605669103 (2006).
14. Yu, K., Li, Q., Shi, G. & Li, N. Involvement of epithelial-mesenchymal transition in liver fibrosis. *Saudi J Gastroenterol* **24**, 5-11, doi:10.4103/sjg.SJG_297_17 (2018).
15. Guz, M. *et al.* Elevated miRNA Inversely Correlates with E-cadherin Gene Expression in Tissue Biopsies from Crohn Disease Patients in contrast to Ulcerative Colitis Patients. *Biomed Res Int* **2020**, 4250329, doi:10.1155/2020/4250329 (2020).
16. Muise, A. M. *et al.* Polymorphisms in E-cadherin (CDH1) result in a mis-localised cytoplasmic protein that is associated with Crohn's disease. *Gut* **58**, 1121-1127, doi:10.1136/gut.2008.175117 (2009).

17. Cunningham, M. F., Docherty, N. G., Burke, J. P. & O'Connell, P. R. S100A4 expression is increased in stricture fibroblasts from patients with fibrostenosing Crohn's disease and promotes intestinal fibroblast migration. *Am J Physiol Gastrointest Liver Physiol* **299**, G457-466, doi:10.1152/ajpgi.00351.2009 (2010).
18. Burke, J. P., Cunningham, M. F., Sweeney, C., Docherty, N. G. & O'Connell, P. R. N-cadherin is overexpressed in Crohn's stricture fibroblasts and promotes intestinal fibroblast migration. *Inflamm Bowel Dis* **17**, 1665-1673, doi:10.1002/ibd.21543 (2011).
19. Yang, J. X., Rastetter, R. H. & Wilhelm, D. Non-coding RNAs: An Introduction. *Adv Exp Med Biol* **886**, 13-32, doi:10.1007/978-94-017-7417-8_2 (2016).
20. Beermann, J., Piccoli, M. T., Viereck, J. & Thum, T. Non-coding RNAs in Development and Disease: Background, Mechanisms, and Therapeutic Approaches. *Physiol Rev* **96**, 1297-1325, doi:10.1152/physrev.00041.2015 (2016).
21. Fehlmann, T. *et al.* The sncRNA Zoo: a repository for circulating small noncoding RNAs in animals. *Nucleic Acids Res* **47**, 4431-4441, doi:10.1093/nar/gkz227 (2019).
22. Ambros, V. The functions of animal microRNAs. *Nature* **431**, 350-355, doi:10.1038/nature02871 (2004).
23. Zhang, X., Hong, R., Chen, W., Xu, M. & Wang, L. The role of long noncoding RNA in major human disease. *Bioorg Chem* **92**, 103214, doi:10.1016/j.bioorg.2019.103214 (2019).
24. Paraskevopoulou, M. D. & Hatzigeorgiou, A. G. Analyzing MiRNA-LncRNA Interactions. *Methods Mol Biol* **1402**, 271-286, doi:10.1007/978-1-4939-3378-5_21 (2016).
25. Wang, H. *et al.* Pro-inflammatory miR-223 mediates the cross-talk between the IL23 pathway and the intestinal barrier in inflammatory bowel disease. *Genome Biol* **17**, 58, doi:10.1186/s13059-016-0901-8 (2016).
26. Spencer, D. M., Veldman, G. M., Banerjee, S., Willis, J. & Levine, A. D. Distinct inflammatory mechanisms mediate early versus late colitis in mice. *Gastroenterology* **122**, 94-105, doi:10.1053/gast.2002.30308 (2002).
27. Lee, J. M., Dedhar, S., Kalluri, R. & Thompson, E. W. The epithelial-mesenchymal transition: new insights in signaling, development, and disease. *J Cell Biol* **172**, 973-981, doi:10.1083/jcb.200601018 (2006).
28. Radisky, D. C. Epithelial-mesenchymal transition. *J Cell Sci* **118**, 4325-4326, doi:10.1242/jcs.02552 (2005).
29. Yang, Y. M. & Yang, W. X. Epithelial-to-mesenchymal transition in the development of endometriosis. *Oncotarget* **8**, 41679-41689, doi:10.18632/oncotarget.16472 (2017).
30. Moreno-Amador, J. L. *et al.* Epithelial to mesenchymal transition in human endocrine islet cells. *PLoS One* **13**, e0191104, doi:10.1371/journal.pone.0191104 (2018).
31. Wu, C. *et al.* DAXX inhibits cancer stemness and epithelial-mesenchymal transition in gastric cancer. *Br J Cancer* **122**, 1477-1485, doi:10.1038/s41416-020-0800-3 (2020).

32. Grande, M. T. *et al.* Snail1-induced partial epithelial-to-mesenchymal transition drives renal fibrosis in mice and can be targeted to reverse established disease. *Nat Med* **21**, 989-997, doi:10.1038/nm.3901 (2015).
33. Latella, G., Di Gregorio, J., Flati, V., Rieder, F. & Lawrance, I. C. Mechanisms of initiation and progression of intestinal fibrosis in IBD. *Scand J Gastroenterol* **50**, 53-65, doi:10.3109/00365521.2014.968863 (2015).
34. Stone, R. C. *et al.* Epithelial-mesenchymal transition in tissue repair and fibrosis. *Cell Tissue Res* **365**, 495-506, doi:10.1007/s00441-016-2464-0 (2016).
35. Mirza, A. H. *et al.* Transcriptomic landscape of lncRNAs in inflammatory bowel disease. *Genome Med* **7**, 39, doi:10.1186/s13073-015-0162-2 (2015).
36. Leng, X. *et al.* LINC01272 Promotes Migration and Invasion of Gastric Cancer Cells via EMT. *Onco Targets Ther* **13**, 3401-3410, doi:10.2147/OTT.S242073 (2020).
37. Wang, S. *et al.* KIF9AS1, LINC01272 and DIO3OS lncRNAs as novel biomarkers for inflammatory bowel disease. *Mol Med Rep* **17**, 2195-2202, doi:10.3892/mmr.2017.8118 (2018).
38. He, Z., Yan, T., Yuan, Y., Yang, D. & Yang, G. miRNAs and lncRNAs in Echinococcus and Echinococcosis. *Int J Mol Sci* **21**, doi:10.3390/ijms21030730 (2020).
39. Lai, X. N. *et al.* MiRNAs and LncRNAs: Dual Roles in TGF-beta Signaling-Regulated Metastasis in Lung Cancer. *Int J Mol Sci* **21**, doi:10.3390/ijms21041193 (2020).

Tables

Table 1 Clinical characteristics of patients

Characteristics	Normal Control	Crohn's Disease
	(n=30)	(n=30)
Gender		
male	17	18
female	13	12
Mean age, years±SD	30.38 ± 9.24	31.45 ± 10.16
Mean duration of disease, years±SD	–	
Disease distribution		
Ileal	–	6
Colonic	–	8
Ileo-colonic	–	15
Peri-ana	–	1
Medications		
Mesalamine	–	7
Antibiotics	–	9
Steroids	–	8
Immunomodulators	–	6

Table2 Primer sequences used for qRT-PCR

Genes		Primer sequences (5’-3’)
Hsa-LINC01272	Forward	CCAAGGTCACGCAGCACAGTC
	Reverse	GCAGAGATGAGCAGCAGTGGTG
Has-GAPDH	Forward	GGTGAAGGTCGGAGTCAACG
	Reverse	CAAAGTTGTCATGGATGHACC
Hsa-miR-153-3p	Forward	GCCGGGCTTGCATAGTCACAA
Has-U6	Forward	CGCTTCGGCAGCACATATAC
Rno-miR-153-3p	Forward	TTGCATAGTCACAAAAGTGATCG
	Reverse	GTGTCGTGGAGTCGGCAA
Rno-E-cadherin	Forward	GGTGAATTTTTAGTTAATTAGCGGTAC
	Reverse	CATAACTAACCGAAAACGCCG
Rno-collagen I	Forward	TGCTGCCTTTTCTGTTCCTT
	Reverse	AAGGTGCTGGGTAGGGAAGT
Rno-collagen III	Forward	GAGGAATGGGTGGCTATCCG
	Reverse	TTGCGTCCATCAAAGCCTCT
Rno-N-cadherin	Forward	GTGCCATTAGCCAAGGGAATTCAGC
	Reverse	GCGTTCCTGTTCCACTCATAGGAGG
Rno-CK	Forward	CACAAGAAGACACTACGAATC
	Reverse	-ACGACTATGAGGACGAAGA
Rno-α-SMA	Forward	TAGCGAGCATCACTGACA
	Reverse	AACATAGAGCCAAGCAACA
Rno- Fibronectin	Forward	CGAAATCACAGCCAGTAG
	Reverse	ATCACATCCACACGGTAG
Rno-GAPDH	Forward	ACTCACTCTTCTACCTTTGATGCT
	Reverse	TGTTGCTGTAGCCAAATTCA

Figures

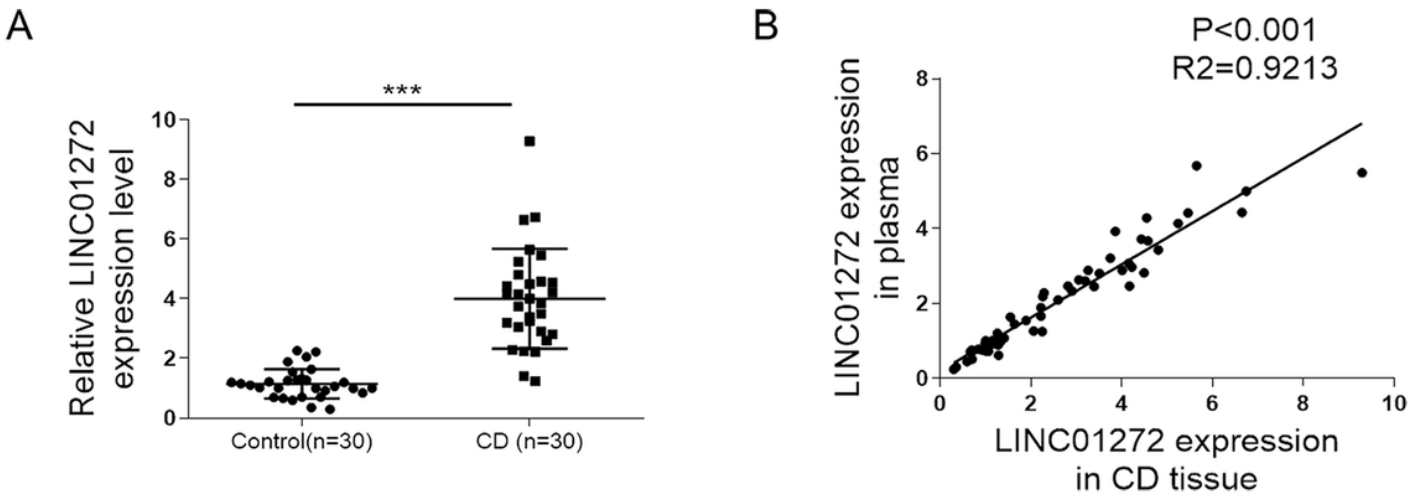

Figure 1

LINC01272 is highly expressed in CD. (A) The relative expression of LINC01272 in control group and CD group. (B) Correlation analysis of the expression of LINC01272 in CD tissues and plasma samples. ***P<0.001.

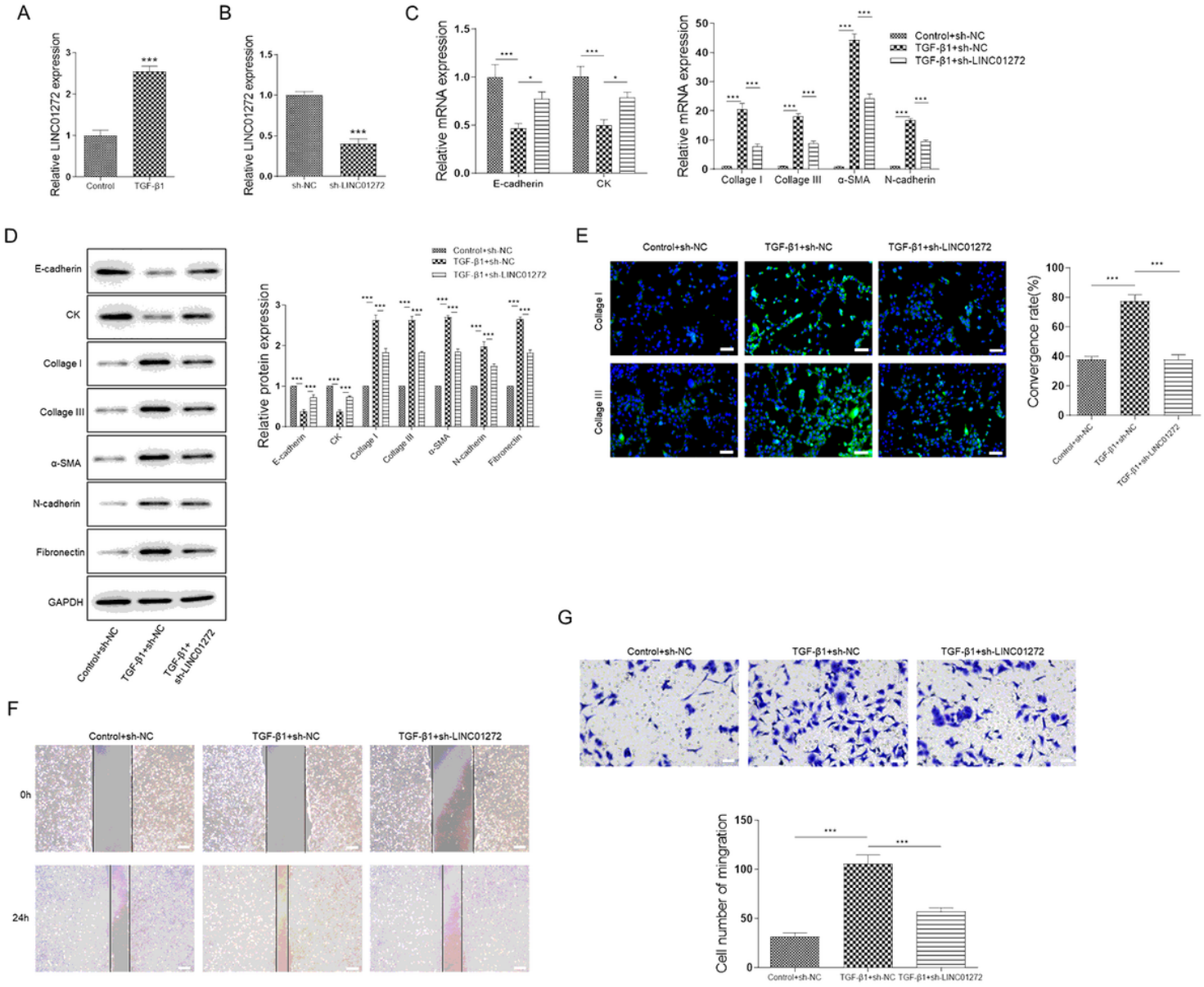

Figure 2

Knockdown of LINC01272 inhibits TGF-β1-induced EMT in IEC-6 cell. (A) Relative expression of LINC01272 in TGF-β1 treated IEC-6 cells detected by qRT-PCR. (B) The transfection efficiency of sh-LINC01272 detected by qRT-PCR. (C) Relative expression of E-cadherin, CK, collagen I, collagen III, α-SMA and N-cadherin mRNA detected by qRT-PCR. (D) Expression of E-cadherin, CK, collagen I, collagen III, α-SMA and N-cadherin protein detected by Western blot. (E) Expression of collagen I, collagen III detected by immunofluorescence. (F) Cell migration ability detected by wound-healing assay. (G) Cell invasion ability detected by transwell assay. *P<0.05, ***P<0.001.

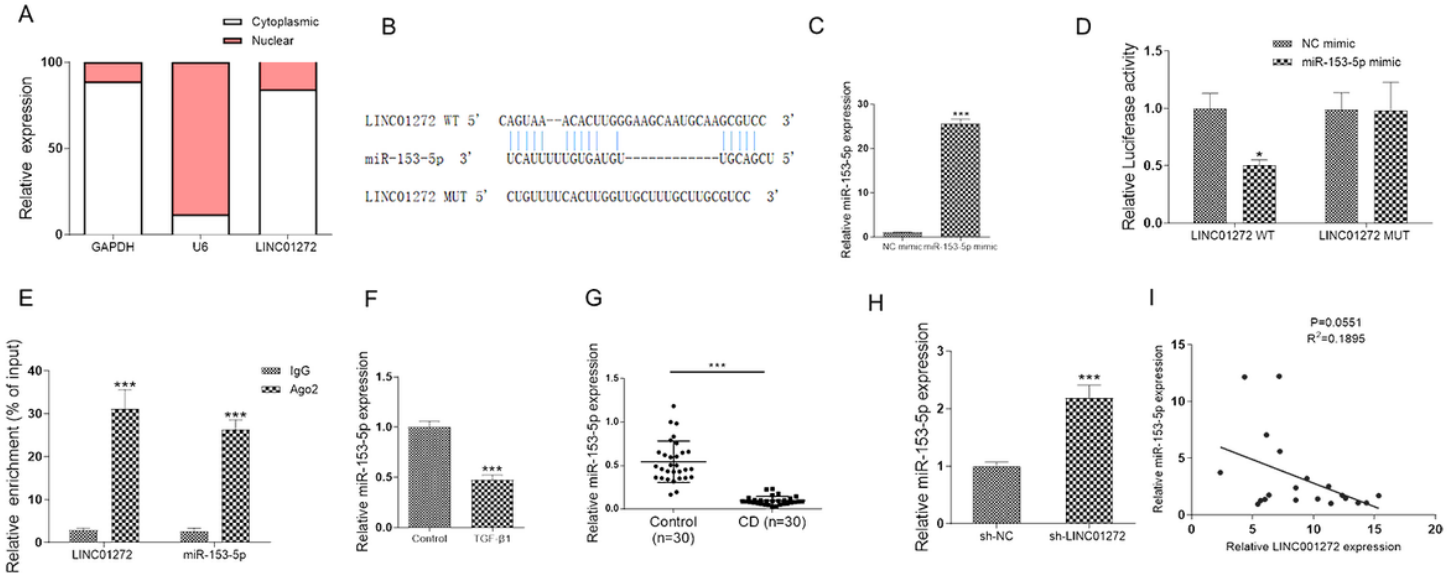

Figure 3

MiR-153-5p targets 3' UTR of LINC01272. (A) Subcellular localization experiment. (B) Targeting relationship between LINC01272 and miR-153-3p predicted by bioinformatics. (C) The transfection efficiency detected by qRT-PCR. (D) Luciferase report experiment verified the relationship between LINC01272 and miR-153-3p. (E) RNA binding protein immunoprecipitation experiment verified the relationship between LINC01272 and miR-153-3p. (F) Relative expression of miR-153-3p in TGF-β1 treated IEC-6 cells. (G) Relative expression of miR-153-3p in control group and CD group. (H) Relative expression of miR-153-3p before and after silencing of LINC01272. (I) Pearson's correlation analysis of the relative expression of LINC01272. *P<0.05, ***P<0.001.

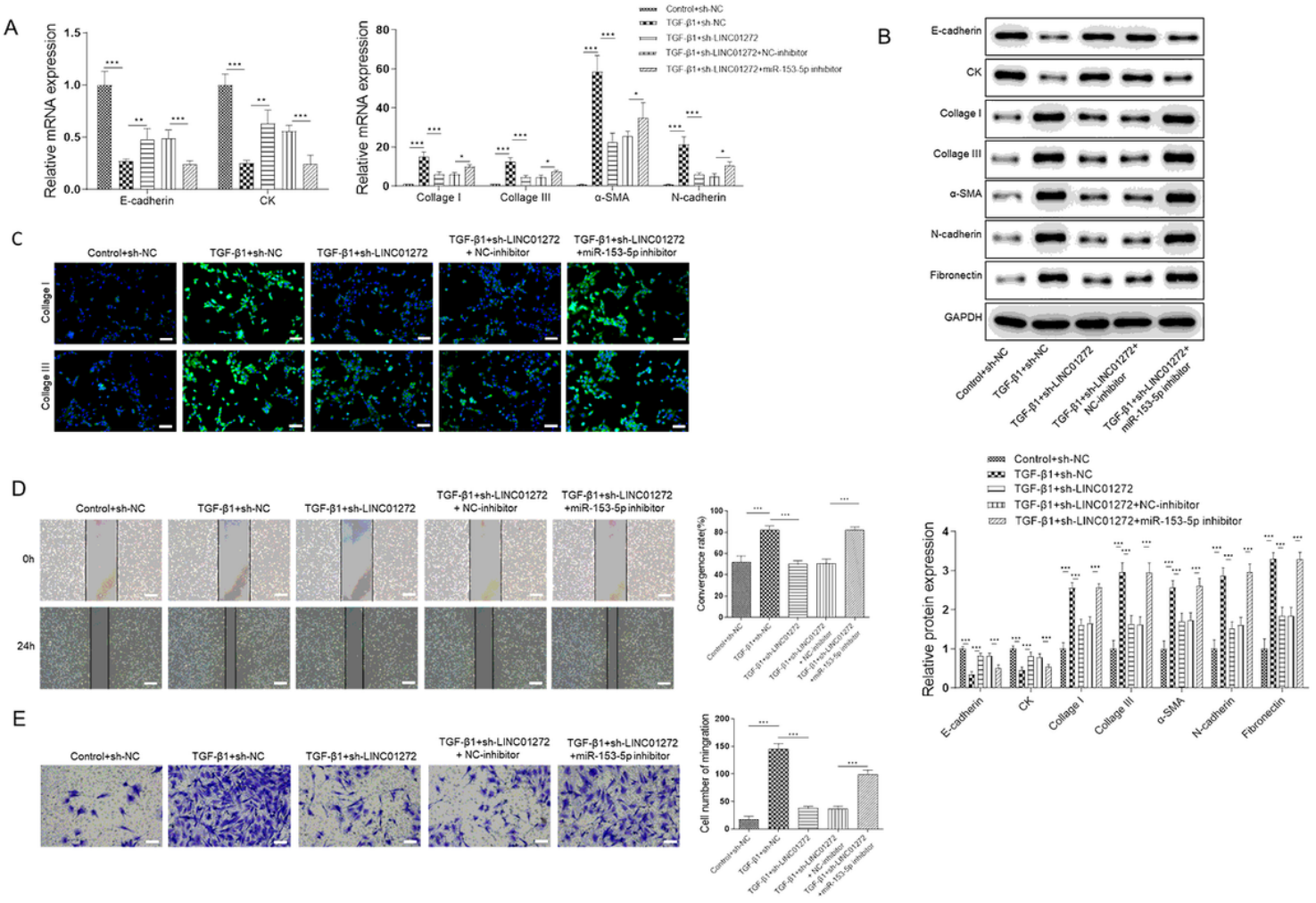

Figure 4

LINC01272 regulates TGF-β1 induced EMT by miR-153-5p axis. (A) Relative expression of E-cadherin, CK, collagen I, collagen III, α-SMA and N-cadherin mRNA detected by qRT-PCR. (B) Expression of E-cadherin, CK, collagen I, collagen III, α-SMA and N-cadherin protein detected by Western blot. (C) Expression of collagen I, collagen III detected by immunofluorescence. (D) Cell migration ability detected by wound-healing assay. (E) Cell invasion ability detected by transwell assay. *P<0.05, **P<0.01, ***P<0.001.

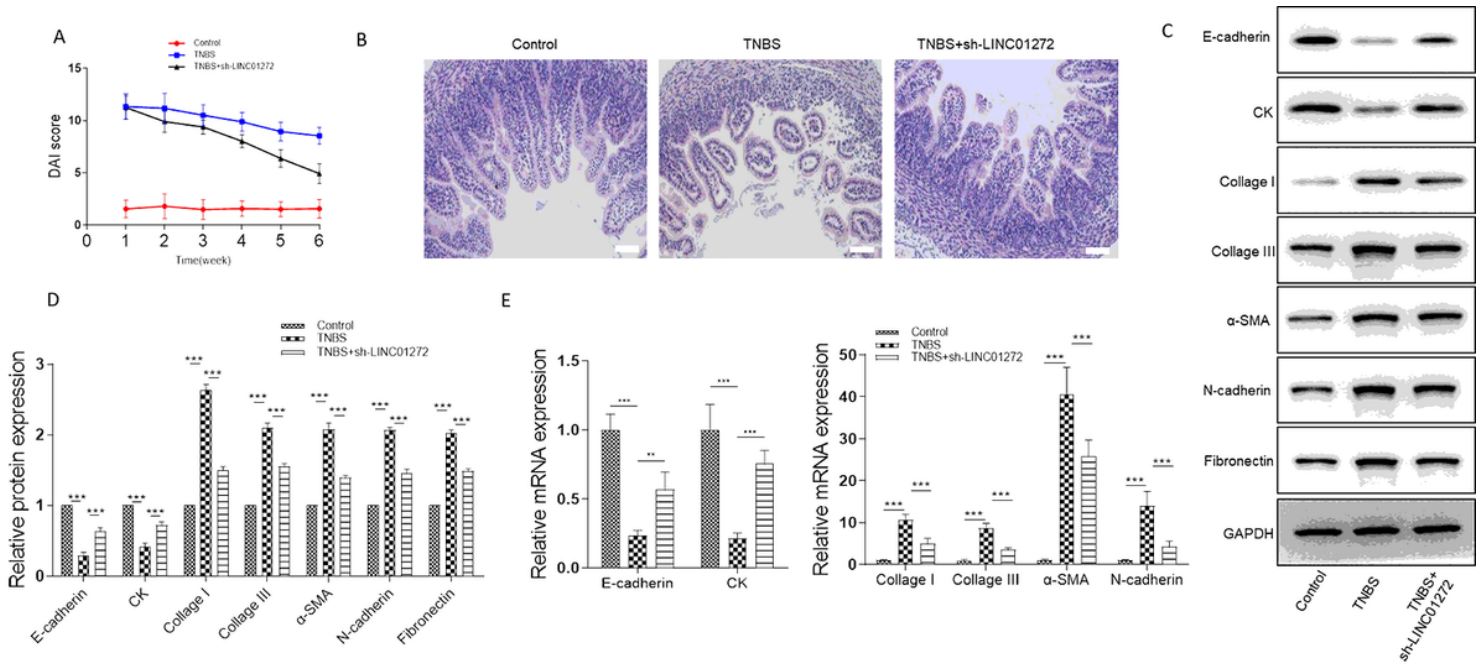

Figure 5

Knockdown of LINC01272 inhibits EMT in the CD mice in vivo. (A) DAI score of control group, TNBS group and TNBS+sh-LINC01272 group. (B) Pathological manifestations of colon tissue of mice in each group. (C-D) Protein levels of EMT-related protein and fibrosis protein in each group of mice. (E) The mRNA of EMT-related protein and fibrosis protein in each group of mice. **P<0.01, ***P<0.001.